

Extended D₂CO emission: The smoking gun of grain surface-chemistry

C. Ceccarelli^{1,2}, L. Loinard³, A. Castets¹, A. G. G. M. Tielens⁴, E. Caux⁵, B. Lefloch², and C. Vastel⁵

¹ Observatoire de Bordeaux, BP 89, 33270 Floirac, France

² Laboratoire d'Astrophysique, Observatoire de Grenoble, BP 53, 38041 Grenoble Cedex 09, France

³ Instituto de Astronomía, UNAM, Apdo Postal 72-3 (Xangari), 58089 Morelia, Michoacán, México

⁴ SRON, PO Box 800, 9700 AV Groningen, The Netherlands

⁵ CESR CNRS-UPS, BP 4346, 31028 Toulouse Cedex 04, France

Received 20 February 2001 / Accepted 23 March 2001

Abstract. We present new observations of the H₂CO and D₂CO emission around IRAS16293-2422, a low mass protostar in the ρ Ophiuchus complex. Bright H₂CO and D₂CO emission is detected up to 40'' from the center, corresponding to a linear distance of \sim 5000 AU. The derived H₂CO abundance profile has two jumps at $r \leq 150$ AU and $r \leq 700$ AU, where the dust temperature reaches 100 K and 50 K respectively. The measured [D₂CO]/[H₂CO] abundance ratio in the envelope is between 0.03 and 0.16, an extremely high value. We demonstrate that the present new observations can only be explained if the D₂CO (and H₂CO) are formed during the previous cold pre-collapse phase, stored in the grain mantles, and released in the gas phase during the pre-collapse phase. We consider the two main competing theories for mantle formation, i.e. pure accretion against grain surface chemistry, and we conclude that the former theory cannot explain the present observations, whereas grain active chemistry very naturally does. We found that the mantles are evaporated because of the thermal heating of the grains by the central source and that in the outer cold envelope H₂CO and D₂CO molecules are embedded in CO-rich mantles which sublimate when the dust is warmer than 25 K. Finally, the present day H₂CO and D₂CO abundances very probably reflect the mantle composition. We argue that mantles have likely formed in an onion-like structure with the innermost ice layers more enriched in H₂CO molecules and we give estimates of the CO hydrogenation efficiency across the envelope and/or in different ices.

Key words. ISM: abundances – ISM: molecules – stars: formation – ISM: individual: IRAS 16293–2422

1. Introduction

Doubly deuterated formaldehyde was discovered towards Orion by Turner (1990). The measured [D₂CO]/[H₂CO] abundance ratio \sim 0.3% made Turner claim that the formaldehyde is mainly synthesized on the grain surface. Subsequently Ceccarelli et al. (1998) and Loinard et al. (2000; hereinafter LCCT2000) discovered an even larger [D₂CO]/[H₂CO] ratio, \sim 5% toward the solar type protostar IRAS16293-2422 (hereinafter IRAS16293) and \sim 26% toward the younger protostar 16293E (Loinard et al. 2001). As in the case of Orion, the large [D₂CO]/[H₂CO] abundance ratio was interpreted as proof that D₂CO is formed on the grain surfaces during the cold and dense pre-collapse phase and released in the gas phase because of the heating of the dust during the collapse. These first works implicitly assumed that the D₂CO line is emitted either in the innermost warm regions close to the central

object, where the dust temperature reaches the ice evaporation temperature (\sim 80 K for H₂O ices), or in shocks associated with the outflow emanating from the young source, where the mantle molecules are sputtered into the gas phase. However, LCCT2000, analyzing the absorption of the D₂CO and H₂CO lines observed towards IRAS16293, found that between us and the source there must be an absorbing layer of H₂CO and D₂CO gas. This gas is relatively cold (\sim 20 K) and enriched in D₂CO. We estimated that the [D₂CO]/[H₂CO] abundance ratio in this gas is \sim 12%; i.e. even larger than the ratio observed towards the source itself (LCCT2000).

In order to clarify the situation we obtained a map of the D₂CO emission around IRAS16293. Our goal was to determine the region where the D₂CO line is emitted and to understand the origin of this emission. The outline of the paper is the following: after reviewing the source background in Sect. 2, we present the new observations in Sect. 3. The discussion and implications of these new observations are reported in Sects. 4 and 5.

Send offprint requests to: C. Ceccarelli,
e-mail: ceccarel@observ.u-bordeaux.fr

2. Source background

IRAS16293 is a 15 L_{\odot} protostar embedded in the small molecular cloud L1689N, in the ρ Ophiuchus complex at 120 pc of distance (Knude & Hog 1998). The gas in L1689N seems to be anomalously deficient in CO (by about a factor ten with respect to the usual assumed CO abundance in clouds) and overabundant in atomic oxygen (Caux et al. 1999). IRAS16293 has been the target of several studies, triggered by the claim of Walker et al. (1986) that the envelope around IRAS16293 is collapsing towards the center (see also Zhou et al. 1995; Narayanan et al. 1998). IRAS16293 has been classified as a Class 0 source (André et al. 1993) and it is very probably in a very early stage of its evolution (Bontemps et al. 1996; Saraceno et al. 1996). An unbiased line survey in the 215 and 350 GHz bands showed the existence of several components in a 30'' region centered on IRAS16293 (Blake et al. 1994; van Dishoeck et al. 1995): an ambient molecular core, a rotating and infalling envelope, an outer cold disk, two warm circumstellar disks and finally a multiple outflow. The outflows have been traced in several molecular species: CO (Walker et al. 1986; Mizuno et al. 1986), O (Ceccarelli et al. 1997), SiO (Hirano et al. 2000). Recently Castets et al. (2001) obtained large scale maps of H₂CO, SiO and O emission. All these tracers give a well defined picture of three outflows emanating from the three sources housed in L1689N (Castets et al. 2001). The structure (i.e. the density and temperature profiles as well as the abundances of the main gas coolants) of the envelope surrounding IRAS16293 has been recently reconstructed based on multifrequency H₂O, SiO, O, and H₂CO line observations (Ceccarelli et al. 2000a,b). The envelope is formed by gas, whose abundance is similar to typical molecular cloud abundances in the outer regions (≥ 150 AU). In the inner regions (≤ 150 AU) the abundances of H₂O, SiO and H₂CO jump to abundances typical of the hot cores of massive protostars. Finally, there is additional evidence that heavier and more complex molecules are also present in this hot-core like region (Ceccarelli et al. 2000c).

3. Observations and results

Using the IRAM 30 meter telescope, we obtained 60'' \times 80'' maps of the D₂CO 4_{0,4}–3_{0,3} (at 231.410 GHz) and H₂CO 3_{1,3}–2_{1,2} (at 211.211 GHz) emission around IRAS16293. Smaller maps of the central 30'' \times 30'' region were obtained in the D₂CO 4_{1,4}–3_{1,3} and 2_{1,2}–1_{1,1} (at 221.192 and 110.837 GHz respectively) transitions. In addition we observed the H₂¹³CO 3_{1,3}–2_{1,2} (at 206.132 GHz) transition towards the central position and towards two other positions offset by (0'', –10'') and (–10'', –10'') respectively. Finally, we observed the H₂CO 2_{1,2}–1_{1,1} (at 140.839 GHz) transition towards the position at offset (0'', –20''), with the goal of measuring the gas temperature at this position (see below).

The observations were performed in January 1999 and August 2000. The telescope beam efficiencies and

beamwidth at 3 mm and 1.3 mm are equal to 0.8 and 0.48, and 22'' and 11'' respectively. The four receivers were connected to units of the autocorrelator set to provide spectral resolutions of 40 and 80 kHz at 110 and 230 GHz respectively. All frequencies of interest here the velocity resolutions are of the order of 0.1 km s^{–1}. The map spacing is 10''. All observations were performed in the position switching mode with an OFF position offset equal to (–180'', 0''). Typical integration times at each position are of few minutes for the H₂CO lines and up to 1 hour for the D₂CO lines.

Figures 1 and 2 show the maps of the integrated intensity $\int T_{\text{mb}} \Delta v$ of the D₂CO 4_{0,4}–3_{0,3} and H₂CO 3_{1,3}–2_{1,2} lines respectively. The D₂CO 4_{1,4}–3_{1,3} and 2_{1,2}–1_{1,1} maps are similar to the 4_{0,4}–3_{0,3} map in the central region and therefore are not shown. We detected H₂¹³CO 3_{1,3}–2_{1,2} emission only towards the central position (see LCCT2000); in the two other observed positions we obtained upper limits to the peak $T_{\text{mb}} \leq 0.03$ K.

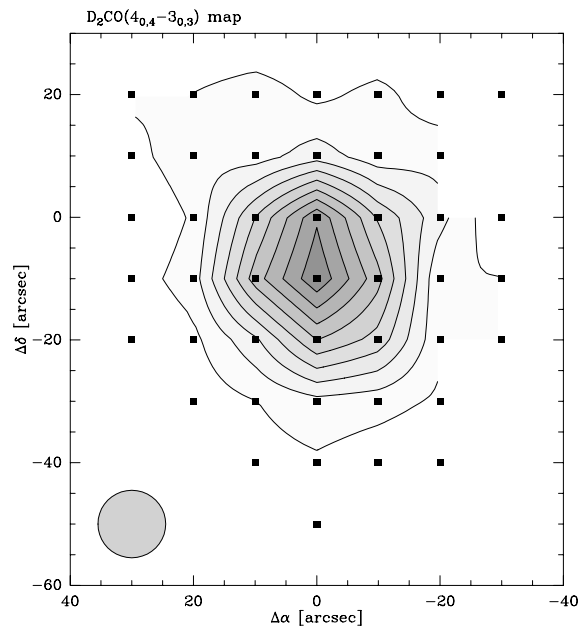


Fig. 1. D₂CO: 4_{0,4}–3_{0,3} line intensity $\int T_{\text{mb}} \Delta v$, integrated over the –20 to +25 km s^{–1} velocity interval. Contour levels start at 0.3 K km s^{–1} and increase by steps of 0.3 K km s^{–1}. The last contour is 2.7 K km s^{–1} and the highest value is 2.95 K km s^{–1}. The (0'', 0'') position corresponds to $\alpha(2000) = 16^{\text{h}}24^{\text{m}}22^{\text{s}}.6$, $\delta(2000) = -24^{\circ}28'33''.0$.

Both H₂CO and D₂CO emission is extended over the observed region. The H₂CO line traces the envelope that surrounds IRAS1629, slightly elongated towards the south (see van Dishoeck et al. 1995; Castets et al. 2001). The H₂¹²CO line opacities derived from the H₂¹³CO observations are relatively small: at the central position, where the absorption is stronger, $\tau \sim 1$ (LCCT2000), while at the two other observed positions τ is less than unity.

Surprisingly, the D₂CO emission is extended ~40'' towards the South. It seems to peak some 10'' South

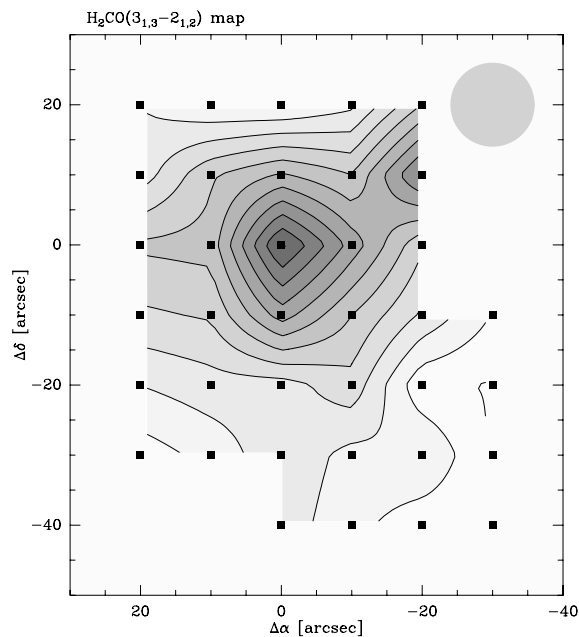


Fig. 2. H₂CO: 3_{1,3}–2_{1,2} line intensity $\int T_{\text{mb}} \Delta v$, integrated over the -20 to $+25$ km s⁻¹ velocity interval.

of the source center, although the difference in the line intensity in the two points is only 20% and therefore only marginally significant. The linewidth is somewhat larger (~ 5 km s⁻¹) towards the center than in the remaining positions, where the D₂CO line is narrow (~ 2 km s⁻¹). This is qualitatively consistent with the picture of D₂CO emission originating in the envelope surrounding IRAS16293 and collapsing towards the center (Ceccarelli et al. 2000a,b). The observations toward the central position would intercept both the relatively static outer envelope and the innermost collapsing regions, giving rise to an enlarged line profile, while the observations in the other positions only intercept the static outer envelope.

Finally, the H₂CO multifrequency observations at the position ($0''$, $-20''$) from the center give a rotational temperature of 25 K (see LCCT2000 for a discussion of how this value is computed).

4. Discussion

4.1. The H₂CO extended emission

In Ceccarelli et al. (2000a; hereinafter CCC2000) and Ceccarelli et al. (2000b; hereinafter CLC2000) we used the observed H₂O, SiO, H₂CO and atomic oxygen lines to reconstruct the physical structure of the envelope surrounding IRAS16293, i.e. the density and temperature profiles as well as the H₂CO abundance profile. To help the reader follow the discussion, Fig. 3 reports the CCC2000 results together with some independent estimates of the gas density and temperature at different distances from the center, which all agree with the CCC2000 model predictions. Specifically, the CLC2000 model predicts that the H₂CO

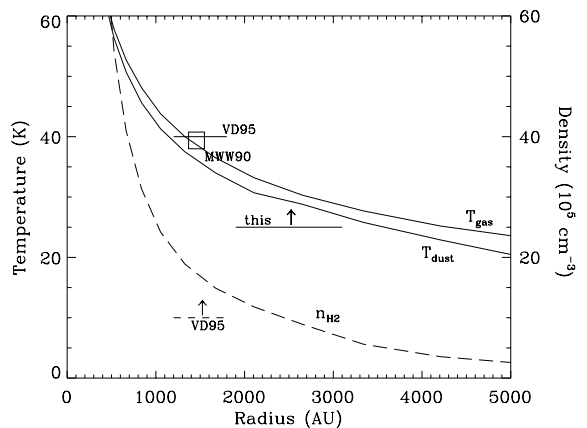


Fig. 3. Profiles of the dust and gas (solid lines) temperatures, and of the gas density (dashed line) as function of the distance from the center, as computed by the CCC2000 model. Note that the density is in 10^5 cm⁻³ units, as marked the right y -axis. The square shows the estimate of the gas temperature by Mundy et al. (1990); the lines marked VD95 are the temperature and density estimates by van Dishoeck et al. (1995); the lower limit marked “this” is this work.

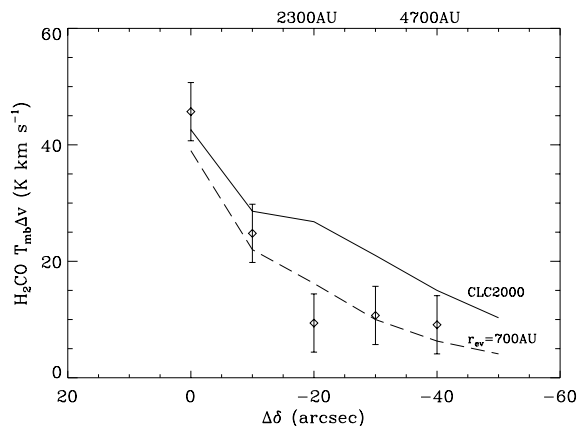


Fig. 4. Profiles of the H₂CO $\int T_{\text{mb}} \Delta v$ line intensity as function of the distance from the center: diamonds show the observations, solid line the CLC2000 model predictions and the dashed line a model with a decrease of the H₂CO abundance outside $r_{\text{ev}} = 700$ AU. In the upper panel we report the linear distance in AU, i.e. $20'' = 2300$ AU and $40'' = 4700$ AU.

abundance is $\sim 10^{-9}$ in the outer cold envelope and 100 times higher in the “hot-core” like region at 150 AU. We emphasize that the model predictions are based on multifrequency H₂CO observations *towards the central position*, i.e. the present new observations are an independent test to this model. The CLC2000 model predicts that the H₂CO 3_{1,3}–2_{1,2} emission extends about 4000 AU, in rough agreement with our present observations. Figure 4 shows the cross scan of the observed $\int T_{\text{mb}} \Delta v$ along the North-South direction and the emission predicted by the CLC2000 model. The comparison between the observed and predicted line intensity suggests that the H₂CO abundance varies as function of the radius also in the outer envelope. In fact, a better fit to the observations is obtained if the H₂CO abundance is 4×10^{-9} at ≥ 700 AU, when the

dust exceeds 50 K, and 4×10^{-10} at larger distances. Both the H₂CO abundance values and where the jump occurs are rather well constrained by the present observations. Incidentally, the new proposed model fits all the previous H₂CO observations towards the central position, as does the CLC2000 model. In effect, the IRAS16293 envelope consists of three regions:

- i) $r \leq 150$ AU: a *hot core like region*, where the dust temperature exceeds 100 K;
- ii) $150 \leq r \leq 700$ AU: a *warm envelope*, where the dust temperature is between 50 K and 100 K;
- iii) $r \geq 700$ AU: a *cold envelope*, where the dust temperature is colder than 50 K.

In the hot core and warm envelope regions the gas phase H₂CO abundance is dominated by mantle desorption.

4.2. The D₂CO extended emission

In LCCT2000 we analyzed six transitions of H₂CO, H₂¹³CO and D₂CO respectively to derive the average rotational temperature (45 K) and H₂CO column density (3.8×10^{14} cm⁻²) towards the central position. The derived [D₂CO]/[H₂CO] ratio, corrected for the H₂CO line opacities, is 0.05 ± 0.01 .

The two H₂CO and D₂CO transitions that we used for the maps shown in Sect. 3 have similar upper level energies (~ 20 cm⁻¹). Because the lines are essentially optically thin, this implies that both lines are excited at approximately the same temperature and density and therefore we can consider their $\int T_{\text{mb}} \Delta v$ ratio as a measure of the [D₂CO]/[H₂CO] abundance ratio in the mapped region. Figure 5 shows the [D₂CO]/[H₂CO] abundance ratio, as derived from the $\int T_{\text{mb}} \Delta v$ line ratio. The [D₂CO]/[H₂CO]

than unity, except in the central position. As already noticed in our previous works (Ceccarelli et al. 1998 and LCCT2000) the observed [D₂CO]/[H₂CO] value ≥ 0.03 is extremely high.

4.3. Origin of deuteration

One key question is: *what causes the observed high degree of deuteration of the gaseous formaldehyde?* In principle, there are two possibilities: either abundant D₂CO is formed *now* by chemical reactions in the gas phase or it was formed *previously* in the colder and denser pre-collapse phase, stored in the grain mantles, and released in the gas phase now, during the collapse. As already argued in our previous works (Ceccarelli et al. 1998; LCC2000; Loinard et al. 2001), it is very unlikely that D₂CO is a present-day gas phase product. The observation of a large deuteration at $\sim 20''$, where the gas temperature is higher than ~ 30 K, strengthens our previous claims. In fact, at such gas temperatures, even the single deuteration of molecules in the gas phase is predicted to be an order of magnitude smaller than that observed by us for D₂CO (e.g. Millar et al. 1989) because of the destruction of H₂D⁺ by H₂ collisions (Watson 1976). Supporting these theoretical arguments, the [DCO⁺]/[HCO⁺] ratio, which traces the [H₂D⁺]/[H₃⁺] ratio, was observed toward IRAS16293 to be 0.009 (van Dishoeck et al. 1995). Likewise, the [DCN]/[HDN] ratio, which ultimately derives from the [CH₂D⁺]/[CH₃⁺] fractionation, observed in IRAS16293 is 0.013 (van Dishoeck et al. 1995). Both these values are an order of magnitude less than the [HDCO]/[H₂CO] ratio (LCCT2000), hence implicating a different origin. *Thus our first conclusion is that the abundant D₂CO observed in the IRAS16293 envelope must have been formed during the pre-collapse phase, stored in the ice grain mantles and released in the gas phase during the collapse.*

There are two competing theories of mantle formation. Either the mantle is formed by mere accretion of molecules synthesized in the gas phase (e.g. Roberts & Millar 2000) or molecules are formed via active grain chemistry on the grain surfaces themselves (e.g. Tielens & Hagen 1982). The first theory predicts high molecular deuteration when the gas is strongly depleted of CO (e.g. Brown & Millar 1989; Willacy & Millar 1998; Roberts & Millar 2000). Recently Roberts & Millar (2000) argued that the [D₂CO]/[H₂CO] abundance ratio can reach 10% when CO is depleted by at least a factor 30 (see their Fig. 10). The problem with this interpretation is that, given the required high depletion, the highly deuterated gas accreting into the mantles would be a small fraction of the total accreted material, reducing the fractionation of the observed evaporated molecules. Conversely, active grain chemistry offers a simple and more viable explanation. Models of grain surface chemistry predict in a natural way high deuteration and high double deuteration of formaldehyde (Tielens 1983; Charnley et al. 1997). In these models, H₂CO and D₂CO are formed via hydrogenation of the CO on the

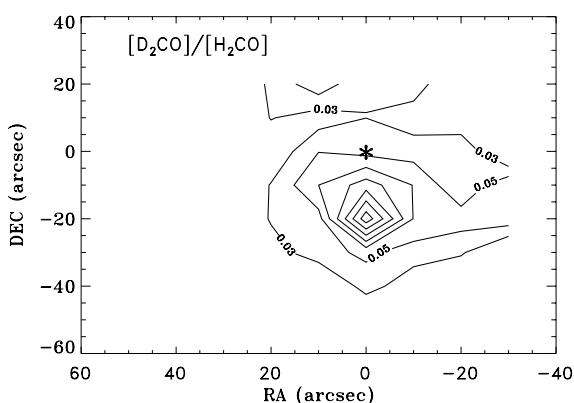


Fig. 5. [D₂CO]/[H₂CO] abundance ratio. Contour levels start at 0.03 and increase by steps of 0.02. The highest value is 0.16 measured at (0'', -20'').

abundance ratio has a peak at (0'', -20''), where it reaches the value 0.16, and then it decreases outwards to 0.03 at (0'', -40''), the last point where we detected D₂CO emission. It is very unlikely that opacity effects can really reverse this trend, since the H₂CO line opacity is less

grain mantles. The molecular fractionation is set by the atomic [D]/[H] ratio in the gas phase at the moment of the mantle formation. This ratio can reach unity in dense ($\geq 10^5 \text{ cm}^{-3}$) gas and hence a relatively high fractionation can be achieved (Tielens 1983). *Hence our second conclusion is that the high abundance of H₂CO, HDCO, and D₂CO in the envelope surrounding IRAS16293 supports models in which – in a previous cold, dark cloud phase – accreted atoms and molecules react on grain surfaces to form hydrogenated (and oxidized) species such as H₂CO and their deuterated counterparts.*

4.4. Mantle desorption

Now the second question is: *what causes the desorption of the grain mantles at distances up to $\sim 4000 \text{ AU}$?*

The comparison between IRAS16293 and the pre-collapse core L1544 can help to enlighten this point. L1544 is a dense ($\sim 10^6 \text{ cm}^{-3}$) and cold ($\sim 10 \text{ K}$) core suspected to be on the verge of collapsing (Tafalla et al. 1998). Caselli et al. (1999) observed a large CO depletion (≥ 10) towards the center of L1544. The density of the IRAS16293 envelope at 3000 AU is $\sim 10^6 \text{ cm}^{-3}$, comparable to the density towards the center of L1544. Observations of H₂CO and D₂CO emission towards this pre-stellar core give an abundance ratio [D₂CO]/[H₂CO] ~ 0.1 (Loinard et al. in preparation), similar to that found in IRAS16293. The H₂CO column density towards L1544 derived by these observations is $\sim 3 \times 10^{12} \text{ cm}^{-2}$. Taking the H₂ column density estimated by Ward-Thompson et al. (1999), $1.3 \times 10^{23} \text{ cm}^{-2}$, gives an H₂CO abundance $\sim 3 \times 10^{-11}$ in L1544. This value is more than ten times smaller than the abundance we measured in the envelope of IRAS16293. This confirms that H₂CO in L1544 is as depleted as CO. But note that although mantles (as seen in the gas phase) seem to have the same D₂CO enrichment in IRAS16293 and L1544, much less of the mantles are found in the gas phase in L1544 than in IRAS16293. Therefore, whereas cosmic rays may be responsible for the partial evaporation of the grain mantles in L1544, a more efficient mechanism evaporates the grain mantles in the envelope of IRAS16293. This mechanism must have to do with the *onset* of the collapse, or more specifically, with the *presence of a protostar inside* the envelope.

Obviously, thermal evaporation of polar ices is excluded, since the dust temperature at 4000 AU is less than the needed 80 K (e.g. Tielens & Allamandola 1987). In principle, a shock associated with the outflow emanating from the central object could cause a partial desorption of the grain mantles. But our observations do not show any evidence of such a shock at the place (south) where we detect abundant D₂CO. On the contrary, an outflow extending in the direction north-east to south-west is well documented in the literature (see Sect. 2), and our D₂CO map does not show any strong emission in that direction. SiO emission maps, believed to trace the shocks in the region strengthen this affirmation. Strong

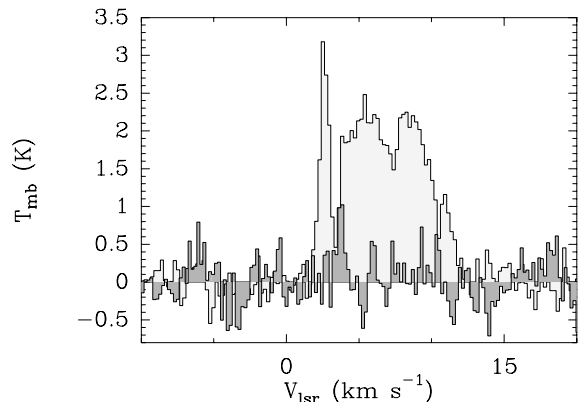


Fig. 6. H₂CO (light grey) and D₂CO (dark grey) line emission at $(-20'', +20'')$ from the center. The H₂CO line profile shows very strong emission between 4 and 12 km s^{-1} , probing the presence of outflowing gas. On the contrary, the outflow is not visible in the D₂CO line.

SiO emission is observed at the CO emission peaks of the outflow where the outflow impacts the surroundings, whereas no trace of SiO emission is observed towards the direction where D₂CO is bright (Hirano et al. 2000; Castets et al. 2001). Actually, the non detection of D₂CO emission at $(-20'', +20'')$, where a bright red wing is observed in H₂CO (Fig. 6) puts a stringent limit to the [D₂CO]/[H₂CO] ratio in this position: ≤ 0.003 .

Accretion shocks may occur along the disk even at thousands of AUs, but they are predicted to be too weak ($\sim 1 \text{ km s}^{-1}$) to cause an appreciable sputtering of the grain mantles. Model computations argue that in order to inject in the gas phase 1% of the mantle, a shock velocity of at least 10 km s^{-1} is needed (e.g. Caselli et al. 1997), which seems very unlikely in this case.

A simple and straightforward explanation of the extended D₂CO emission is that iced H₂CO and D₂CO molecules are embedded in a matrix rich in CO, or other non-polar, volatile molecules, which are evaporated at $\sim 4000 \text{ AU}$, where the dust temperature exceeds 25 K. Analysis of the detailed profile of the solid CO fundamental at $4.67 \mu\text{m}$ have shown that much of the solid CO is in an ice phase, which is non-polar in character; i.e., consists mainly of CO, N₂, and/or O₂ molecules (Tielens et al. 1991; Chiar et al. 1996). This non-polar ice mantle is distinct from the H₂O-rich ice phase which carries the $3.0 \mu\text{m}$ ice band and dominates the global ice composition in molecular clouds. The importance of ice segregation and thermal processing has also been inferred from the analysis of the detailed profiles of the ¹²CO₂ bending mode, the ¹³CO₂ stretching mode and the ¹²CO₂ overtones (Chiar et al. 1998; Boogert et al. 2000). This segregation of ice mantle molecules into components with different volatility is now generally attributed to the heating action as the newly formed central star increases its energy output.

The ensemble of our observations is consistent with the hypothesis that at $\sim 4000 \text{ AU}$ CO-rich mantles evaporate, injecting in the gas phase traces of H₂CO and D₂CO.

For example, the H₂CO abundance in the cold envelope of IRAS16293 is at least four times larger than that measured in L1689N (the cloud hosting IRAS16293), which is $\leq 10^{-10}$ (Castets et al. 2001). Besides, CO itself seems depleted in the L1689N cloud by more than a factor 10 (Caux et al. 1999), whereas no CO depletion is observed towards IRAS16293 (Mundy et al. 1990).

At a somewhat smaller distance, ~ 700 AU, a second layer of the mantle including ten times more H₂CO molecules evaporates: the dust temperature is about 50 K, very close to the 45 K evaporation temperature of pure H₂CO ices (Tielens & Allamandola 1987). Finally at ~ 150 AU a third layer of the mantle, formed mainly by water molecules, evaporates, injecting another factor of 25 more of H₂CO molecules in the gas phase. *Our third conclusion is therefore that thermal heating of the dust releases the grain mantle constituents in the gas phase.* The mantles either have formed in an “onion-like” structure (predominantly H₂O ices covered by H₂CO ices which are themselves coated by predominantly CO ices) or are more enriched in H₂CO molecules going inwards. The observations so far available do not allow us to draw a conclusive picture of the mantle formation. There are several distinct possibilities which could explain the observations. For example, the observed non-polar, CO-rich mantles could be on a separate dust component, e.g. the large grains versus the small grains, due to size-dependent outgassing. It could also be due to a difference in the history of mantles formed in different places in the cloud.

4.5. Mantle formation

Once injected in the gas phase, H₂CO and D₂CO would undergo chemical reactions which may change their initial abundances. Charnley et al. (1992) estimated that the time scale for the conversion of H₂CO first into more complex molecules and then back into CO by gas phase chemical reactions in a dense ($\geq 10^6$ cm⁻³) and hot (≥ 100 K) core is $\geq 10^4$ yr, comparable to the IRAS16293 presumed age¹. Deuterated formaldehyde abundance will also be changed by gas phase reactions on a time scale of $\sim 10^4$ yr (Charnley et al. 1997). Thus, at first approximation, the gas phase H₂CO and D₂CO abundances reflect their mantle abundances. In the previous paragraphs we demonstrated two facts:

- formaldehyde fractionation increases going inwards: outside the envelope it is at least ten times smaller than inside the envelope;
- larger amounts of H₂CO molecules are injected in the gas phase going inwards.

This behavior is qualitatively and quantitatively in agreement with what is expected if H₂CO results from CO hydrogenation on the grain mantles, i.e. with active

grain chemistry model predictions. Charnley et al. (1997) showed that, when the accreting gas is dense ($\geq 10^5$ cm⁻³) $[H]/[CO] \ll 1$, and the mantle $[D_2CO]/[H_2CO]$ abundance ratio depends quadratically on the accreting $[D]/[H]$ ratio, i.e. $[D_2CO]/[H_2CO] \propto ([D]/[H])^2$. On the other hand, the gas phase $[D]/[H]$ ratio depends almost linearly on the density of the gas (e.g. Tielens 1983), which implies that the $[D_2CO]/[H_2CO]$ abundance ratio depends approximatively on the square of the accreting gas density: $[D_2CO]/[H_2CO] \propto n^2$. Applying these results to the IRAS16293 envelope (where $n \propto r^{-3/2}$) gives a $[D_2CO]/[H_2CO]$ abundance ratio which decreases approximately with the cube of the radius r , i.e. $[D_2CO]/[H_2CO] \propto r^{-3}$. This is roughly consistent with our observations which show that the $[D_2CO]/[H_2CO]$ ratio decreases by about a factor of five going from 20'' to 40''. It is also consistent with the observed $[D_2CO]/[H_2CO]$ inside and outside the envelope. In fact, the $[D_2CO]/[H_2CO]$ ratio ≤ 0.003 (Sect. 4.4) outside the envelope (where the density is $\sim 5 \times 10^4$ cm⁻³; Caux et al. 1999), is at least a factor ten lower than the $[D_2CO]/[H_2CO]$ ratio = 0.03 (Sect. 4.2) at the border of the envelope (where the density is $\sim 5 \times 10^5$ cm⁻³).

The fact that the fractionation decreases to 0.05 in the $\leq 20''$ region can be explained by the more efficient protonation, followed by dissociative recombination, of the D₂CO, which proceeds at a rate roughly proportional to the square density.

Finally, the amount of evaporated H₂CO in the three regions we identified (hot core, warm envelope, cold envelope) can be used to estimate the efficiency of CO hydrogenation across the envelope and/or in different ices. Assuming a CO abundance of 10^{-4} , the $[H_2CO]/[CO]$ results are: 10^{-3} in the hot core, 4×10^{-5} in the warm envelope and 4×10^{-6} in the cold envelope. These values reflect the efficiency with which CO is hydrogenated in the ices (Tielens & Hagen 1982): in polar ices (hot core) the efficiency is ~ 250 times higher than in non-polar ices (cold envelope).

5. Conclusions

We presented a $60'' \times 80''$ map around IRAS16293 of the H₂CO and D₂CO line emission. We detected H₂CO and D₂CO emission up to 40'' from the center, corresponding to a linear distance of ~ 5000 AU.

We used the observed H₂CO emission to reconstruct the H₂CO abundance profile across the envelope. We identified three regions:

- in the inner “hot-core like” ($r \leq 150$ AU) region the H₂CO abundance is 10^{-7} , in agreement with our previous claims;
- in the intermediate “warm envelope” ($150 \leq r \leq 700$ AU) region the H₂CO abundance is 4×10^{-9} ;
- in the outer “cold envelope” ($r \geq 700$ AU) region the H₂CO abundance is 4×10^{-10} .

¹ IRAS16293 has at its center a $0.8 M_{\odot}$ protostar accreting at a rate of $3.5 \times 10^{-5} M_{\odot} \text{ yr}^{-1}$ (Ceccarelli et al. 2000a). Assuming that the accretion rate is constant, the age of the protostar is $\sim 2 \times 10^4$ yr.

The measured [D₂CO]/[H₂CO] abundance ratio is 0.03 at the border of the envelope and increases going inwards, with a peak at 20'' where it is 0.16. This extremely high formaldehyde deuteration cannot be a present-day gas phase product. On the contrary, D₂CO must have been formed on the grain mantles during the previous cold *pre-collapse phase* and it has been injected in the gas phase during the warm *collapse phase*. We discussed the possibilities that such mantles are formed because of either pure gaseous D₂CO accretion or D₂CO formation via CO hydrogenation on the grain surfaces. The former theory cannot account for the observed values in a consistent way. In contrast, active grain chemistry successfully accounts for both the absolute observed fractionation and the observed gradient across the envelope.

We demonstrated that mantles are evaporated because of the thermal heating of the grains by the central source. In the “cold envelope” H₂CO and D₂CO molecules are embedded in CO-rich mantles which evaporate when the dust is warmer than ~25 K, at ~4000 AU. In the “warm envelope” a layer of apparently pure H₂CO ice is evaporated and, finally, prevalently H₂O ices are evaporated in the innermost 150 AU region. The measured H₂CO abundances in the three regions have been used to estimate the efficiency of CO hydrogenation across the envelope and/or in different ices. CO is hydrogenated 250 times more efficiently in H₂O-rich ices than in CO-rich ices.

Acknowledgements. It is a pleasure to thank T. J. Millar and E. Bergin for useful discussions on molecular deuteration in the gas phase and mantle accretion. We also thank the referee, E. Herbst, for carefully reading the manuscript.

References

- André, P., Ward-Thompson, & Barsony, M. 1993, *ApJ*, 406, 122
- Blake, G. A., van Dishoeck, E. F., Jansen, D. J., et al. 1994, *ApJ*, 428, 680
- Bontemps, S., André, P., Terebey, S., & Cabrit, S. 1996, *A&A*, 311, 858
- Boogert, A. C. A., Ehrenfreund, P., Gerakines, P. A., et al. 2000, *A&A*, 353, 349
- Brown, P. D., & Millar, T. J. 1989, *MNRAS*, 237, 661
- Castets, A., Ceccarelli, C., Loinard, L., Caux, E., & Lefloch, B. 2001, *A&A*, submitted
- Caselli, P., Hartquist, T. W., & Havnes, O. 1997, *A&A*, 322, 296
- Caselli, P., Walmsley, C. M., Tafalla, M., Dore, L., & Myers, P. C. 1999, *ApJ*, 523, L165
- Caux, E., Ceccarelli, C., Castets, A., et al. 1999, *A&A*, 347, L1
- Ceccarelli, C., Hollenbach, D. J., & Tielens, A. G. G. M. 1996, *ApJ*, 471, 400 (CHT96)
- Ceccarelli, C., Haas, M. R., Hollenbach, D. J., & Rudolph, A. L. 1997, *ApJ*, 476, 771
- Ceccarelli, C., Castets, A., Loinard, L., Caux, E., & Tielens, A. G. G. M. 1998, *A&A*, 338, L43
- Ceccarelli, C., Castets, A., Caux, E., et al. 2000a, *A&A*, 355, 1129
- Ceccarelli, C., Loinard, L., Castets, A., Tielens, A. G. G. M., & Caux, E. 2000b, *A&A*, 357, L9
- Ceccarelli, C., Loinard, L., Castets, A., Faure, A., & Lefloch, B. 2000c, *A&A*, 362, 1122
- Charnley, S. B., Tielens, A. G. G. M., & Millar, T. J. 1992, *ApJL*, 399, L71
- Charnley, S. B., Tielens, A. G. G. M., & Rodgers, S. D. 1997, *ApJ*, 482, L203
- Chiar, J. E., Adamson, A. J., & Whittet, D. C. B. 1996, *ApJ*, 472, 665
- Chiar, J. E., Gerakines, P. A., Whittet, D. C. B., et al. 1998, *ApJ*, 498, 716
- Hirano, N., Mikami, H., Umemoto, T., Yamamoto, S., & Taniguchi, Y. 2000, *ApJ*, in press
- Knude, J., & Hog, E. 1998, *A&A*, 338, 897
- Loinard, L., Castets, A., Ceccarelli, C., Tielens, A. G. G. M., et al. 2000, *A&A*, 359, 1169 (LCCT2000)
- Loinard, L., Castets, A., Ceccarelli, C., Caux, E., & Tielens, A. G. G. M. 2001, *ApJ*, in press
- Millar, T. J., Bennett, A., & Herbst, E. 1989, *ApJ*, 340, 906
- Mizuno, A., Fukui, Y., Iwata, T., Nozawa, S., & Takano, T. 1990, *ApJ*, 356, 184
- Mundy, L. G., Wootten, H. A., & Wilking, B. A. 1990, *ApJ*, 352, 159
- Narayanan, G., Walker, C. K., & Buckley, H. D. 1998, *ApJ*, 496, 292
- Roberts, H., & Millar, T. J. 2000, *A&A*, 361, 388
- Saraceno, P., André, P., Ceccarelli, C., Griffin, M., & Molinari, S. 1996, *A&A*, 309, 827
- Tafalla, M., Mardones, D., Myers, P. C., Caselli, P., Bachiller, R., & Benson, P. J. 1998, *ApJ*, 504, 900
- Tielens, A. G. G. M., & Hagen, W. 1982, *A&A*, 114, 245
- Tielens, A. G. G. M. 1983, *A&A*, 119, 177
- Tielens, A. G. G. M., & Allamandola, L. 1987, in *Interstellar Processes*, ed. D. J. Hollenbach, & H. E. Thronson
- Tielens, A. G. G. M., Tokunaga, A. T., Geballe, T. R., & Baas, F. 1991, *ApJ*, 381, 181
- Turner, B. E. 1990, *ApJ*, 362, L29
- van Dishoeck, E. F., Blake, G. A., Jansen, D. J., & Groesbeck, T. D. 1995, *ApJ*, 447, 760
- Walker, C. K., Lada, C. J., Young, E. T., Maloney, P. R., & Wilking, B. A. 1986, *ApJ*, 309, L47
- Watson, W. D. 1976, *Rev. Mod. Phys.*, 48, 513
- Ward-Thompson, D., Motte, F., & André, P. 1999, *MNRAS*, 305, 143
- Willacy, K., & Millar, T. J. 1998, *MNRAS*, 298, 562
- Zhou, S. 1995, *ApJ*, 442, 685